ARTICLE

Predicting H_2S Oxidative Dehydrogenation over Graphene Oxides from First Principles

Bin Huang*, Bi-bo Chen, Rong Chen

Department of Materials Science and Engineering, East China Institute of Technology, Nanchang 331000, China

(Dated: Received on October 27, 2014; Accepted on March 16, 2015)

Spin-polarized periodic density functional theory was performed to characterize H_2S adsorption and dissociation on graphene oxides (GO) surface. The comprehensive reaction network of H_2S oxidation with epoxy and hydroxyl groups of GO was discussed. It is shown that the reduction reaction is mainly governed by epoxide ring opening and hydroxyl hydrogenation which is initiated by H transfer from H_2S or its derivatives. Furthermore, the presence of another OH group at the opposite side relative to the adsorbed H_2S activates the oxygen group to facilitate epoxide ring opening and hydroxyl hydrogenation. For H_2S interaction with -O and -OH groups adsorption on each side of graphene, the pathway is a favorable reaction path by the introduction of intermediate states, the predicted energy barriers are 3.2 and 10.4 kcal/mol, respectively, the second H transfer is the rate-determining step in the whole reaction process. In addition, our calculations suggest that both epoxy and hydroxyl groups can enhance the binding of S to the C−C bonds and the effect of hydroxyl group is more local than that of the epoxy.

Key words: First principles, H_2S, Adsorption, Dissociation

I. INTRODUCTION

Graphene, a one-atom thick sheet of sp^2 hybridization carbon, forms one of the strongest in-plane bonds among all materials [1–3]. Due to its unique structural, exceptional electronic and mechanical characteristics, graphene has attracted great attention in electrodes, sensors, and hydrogen storage devices. However, only weak adsorption was experimentally and theoretically found among gas molecule with the pristine graphene because of the low adsorption energies of gas molecules on the graphene surfaces. Thus, many theoretical and experimental studies intend to change the chemical properties of carbon nanomaterials by functionalization with other impurities, such as defect and active sites [4–9].

Graphene oxides (GO), the single-layered graphite oxide, in which 2D graphene sheet was aggregated of oxygen functional groups, had attracted many scientists to this research areas [10–15]. GO can be chemically reduced to obtain graphene sheet. Chemical agents, such as hydrazines [16, 17], vitamin C [18], sulfur-containing compounds [19], and hydrogen iodide [20], *etc.* have been used to remove the hydroxyl and epoxy groups in GO. Despite these chemical agents reduction in GO results in sp^2 structure, graphene sheet still leaves a number of defects because reduction process is unable to completely remove all the oxygen functionalities. The remaining oxygen functional groups on GO as the active defective sites were believed to enhance the interaction of molecules with graphene. The reduced graphene oxide, especially chemically converted graphene, can be used as high performance molecular sensors, such as for NO_2 and NH_3 [21].

A series of sulfur-containing compounds such as $NaHSO_3$, Na_2SO_3, Na_2S, $SOCl_2$, and SO_2, were used as reducing agents to reduce graphene oxide to graphene, indicating sulfur-containing compounds are also good reducing agents for the reduction of GO [19]. Graphite oxide as a starting material may be thermally exfoliated in a sulfur-containing gaseous environment, such as SO_2, H_2S, and CS_2 gas atmosphere. Doping of graphene with heteroatoms have long been known as an effective way to bring about a greater effect on the properties of the final product [22]. Sulfur-doped graphene shows excellent electrocatalysis for the oxygen reduction reaction (ORR), which is of high industrial importance, and makes them ideal candidates for metal-free oxygen reduction electrocatalysts [23–32]. Experimentally, Ji *et al.* also demonstrate strong interaction between graphene oxide and sulfur or polysulfides may improve lithium/sulfur cells with a high reversible capacity of 950−1400 (mA·h)/g [25]. In view of these experimental efforts, we believe that the mechanism of H_2S decomposition on GO is important and valuable to

*Author to whom correspondence should be addressed. E-mail: binhuang@xmu.edu.cn, Tel./FAX: +86-791-83896550

be conducted urgently by theoretical studies.

In this work, we performed first-principles computations to explore the detailed adsorption and dissociation mechanisms for the H_2S molecule on graphene oxides. The comprehensive reaction network of H_2S oxidation with epoxy and hydroxyl groups of GO was studied in detail. The results demonstrate that the oxygen-conatining groups in GO may be responsible for reactions with H_2S.

II. COMPUTATIONAL DETAILS

All spin polarization calculations were carried out using DFT code Dmol^3 [33] as implemented in the Material Studio. The local density approximation with Perdew-Wang correlation (PWC) [34] was used to describe the exchange and correlation term during the self-consistent field iterations, and all-electron double numerical basis set with polarization function (the DNP basis set) were chosen for the DFT calculation. Self-consistent field procedures were done with a convergence criterion of 10^{-3} a.u. on the gradient and displacement and 10^{-5} a.u. on the total energy and electron density. To determine the activation energy for reaction path, a transition state connecting two stable structures through a minimum energy path was searched by complete synchronous transit (LST) and quadratic synchronous transit (QST) search methods. The atomic charge distributions were investigated by Hirshfeld population analysis, which has been domenstrated to be a useful tool. The Monkhorst-pack k-point sampling during geometric optimization for the transition state (TS) was 7×7×1.

Although many models of GO have been built in theoretical studies, the structure of GO still remain unclear. Furthermore, the O content of GO can vary greatly, depending on the experimental conditions and the degree of oxidation. To investigate the interaction adsorption and decomposition of H_2S on graphene oxides, we mainly selected -OH and -O- groups on its surface. A hexagonal graphene supercell (4×4 graphene unit cell) containing 32 atoms was built to model a graphene surface, and modulus unit cell vector in the z direction was set to 16 Å, which can render the interactions between the system and their mirror images. Figure 1 shows the optimized geometry of graphene (C32) containing epoxide and hydroxyl groups, respectively. Similar to the previous observed structures of GO, the structure containing the 1,2-hydroxyl group pair at the opposite side (Fig.1(c), denoted as 2OH-2-gr) is the most energetically favorable one in all optimized GO with two hydroxyl functional groups. It is commonly accepted under the O-rich conditions, GO contains more epoxy, whereas under the H-rich conditions, hydrogenated graphene oxides will exist. In the intermediate region, GO usually contains both epoxies (-O-) and hydroxyls (-OH). When graphene oxides contain both OH and O groups (Fig.1 (d) and (e) denoted as

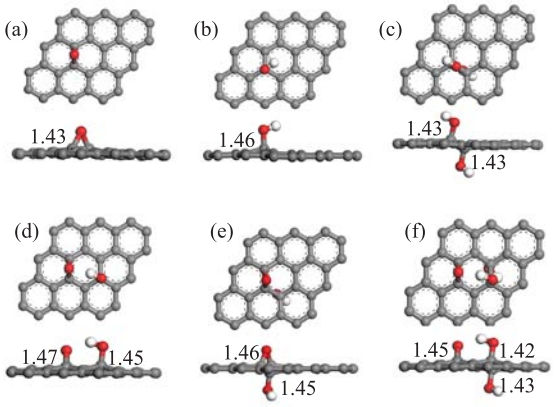

FIG. 1 Top and side view of the geometric structures of oxide graphene. The red, gray, and white balls represent O, C, and H atoms, respectively. Distances are given in Å. (a) O-gr, (b) OH-gr, (c) 2OH-2-gr, (d) O-OH-1-gr, (e) O-OH-2-gr, and (f) O-2OH-gr.

O-OH-1-gr and O-OH-2-gr, respectively), the total energy of O-OH-2-gr is 3.3 kcal/mol in energy lower than that of O-OH-1-gr. The model (Fig.1(f), denoted as O-2OH-gr) was obtained by adding an another -OH to the structure O-OH-2-gr.

Using total energy calculation, the binding energy E_b of H_2S and other containing S species with the GO can be calculated as follows:

$$E_b = E_{GO} + E_{adsorbate} - E_t \quad (1)$$

where E_t, E_{GO}, and $E_{adsorbate}$ denoted the total energies of GO with S species, the energies of each GO model, and the energies of the corresponding adsorbate, respectively. Note that the positive binding energies correspond to exothermicity for adsorption and dissociation of H_2S on GO.

III. RESULTS AND DISSCUSSION

A. Interaction of H_2S with a single functional group on GO

In the previous studies, only weak interaction was obtained in most cases when these molecules interact with pristine graphene nanosheet [35]. Here, we also consider H_2S adsorption on pristine graphene, the optimized results show H_2S molecule parallels graphene surface, the calculated adsorption energy is 1.2 kcal/mol, and charge transfer from H_2S to graphene is 0.002e, which indicate that the relative interaction appears between H_2S and graphene.

Previous experimental and theoretical results present that the metal-doped graphene or reduced graphene oxides are canditates for design of highly sensitive sensors because of the presence of active vacancies provided by the oxygen-containing groups. Morever, the oxygen groups in GO may be triggered for reactions with

DOI:10.1063/1674-0068/28/cjcp1410187

H_2S and covalent C−S bond formation. To fully understand the H_2S dehydrogenation process, it is necessary to calculate the adsorption and decomposition of H_2S with a single functional groups on GO. In Fig.2, the optimized structures, including H_2S-O-gr, SH(A)-O-gr, and SH(B)-O-gr, for the interaction of H_2S with graphene oxides with a single functional groups on GO are presented and the corresponding results are shown in Table I. From Fig.2(a), the H_2S molecule can interact with an epoxide, the distance between the H and O atoms is 2.15 Å and the calculated E_b is about 7.3 kcal/mol, which is greater than 1.2 kcal/mol estimated for the H_2S adsorption on pristine grapheme. It can be understood by electrostatic attraction between a positively charged H (0.053e) in H_2S and the negatively charged O (−0.168e) in epoxide. It might be mentioned that the entropy changes have been applied to describe adsorption behavior during the gas adsorption process. From our calculations, the entropy change (ΔS) is −121.7 J/K during the H_2S adsorption on GO sheet, a negative ΔS value reflects the decreased randomness during adsorption process, thus decrease in the entropy and free energy is the driving force of H_2S adsorption on O-gr. Now we address SH adsorption on GO with epoxide group, we found the ring-opening reaction is attributed to the H atom transfer from H_2S to the epoxy group after adsorption. Obviously, SH species may adsorb on different carbon sites A and B shown in Fig.2 (b) (SH(A)-O-gr) and (c) (SH(B)-O-gr), respectively. The calculated E_b energies for site B (Fig.2(b)) is 7.9 kcal/mol, weaker than site A (14.3 kcal/mol). However, it is worth noting that the direct binding site C (see Fig.2(a)) of SH is energetically unfavorable, which is understandable because the two carbon atoms connecting the formed OH and SH belong to the same sublattice of graphene, resulting in an additional destroying the sublattice balance of graphene [36, 37]. The structures show that the C−S bonds are 1.94 and 1.91 Å for sites A and B, respectively, and OH···S bond between newly generated OH and SH groups is 2.15 Å for site A. The net charge transfer from GO to H_2S after dissociation are in the range of 0.072e to 0.255e.

In similarity, we also took into account the reaction process between H_2S and GO containing two hydroxyl groups. The optimized structures including H_2S-2OH-2, SH(A)-2OH-2, and SH(B)-2OH-2, and binding energy of the involved intermediates are listed in Fig.2 (d)−(f) and Table I, respectively. For the adsorptions of H_2S on 2OH-2-gr (Fig.2(e)), the calculated E_b is 9.3 kcal/mol and the distance between the H and O atoms is 1.95 Å. During the H_2S dissociation on 2OH-2-gr, the H atom abstraction from adsorbed H_2S leading to SH species. Like H_2S dissociation on single epoxide functional, SH also may be bound to different carbon sites A (Fig.2(d)), and B (Fig.2(f)), respectivley. The predicted binding energy for SH(A)-2OH-2 and SH(B)-2OH-2 is 16.0 and 15.1 kcal/mol, respectively. For comparsion, in the H_2S decomposition on GO with single -OH process, we find that obtained SH species can escape without containing oxygen functional on graphene surface due to the only OH hydrogenation, suggesting functional groups on GO may immobilize SH species.

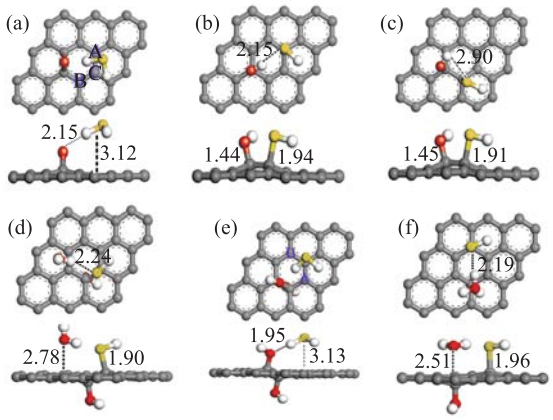

FIG. 2 Top and side view for interaction of H_2S with a single functional groups on GO. The red, gray, yellow, and white balls represent O, C, S, and H atoms, respectively. Distances are given in Å. (a) H_2S-O-gr, (b) SH(A)-O-gr, (c) SH(B)-O-gr, (d) SH(A)-2OH-2, (e) H_2S-2OH-2, and (f) SH(B)-2OH-2.

TABLE I The calculated binding energy (E_b) and main parameters of key adsorbates on graphene oxides with a single functional groups on GO. d represents the shortest distance between the adsorbate and surface graphene, and ΔQ is the charge transfers from the adsorbate to GO.

Structure	Adsorbate	E_b/(kcal/mol)	d/Å	ΔQ/e
H_2S-O-gr	H_2S	7.3	3.12	0.072
SH(A)-O-gr	SH	14.3	1.94	0.233
SH(B)-O-gr	SH	7.9	1.91	0.194
H_2S-2OH-2	H_2S	9.3	3.13	0.061
SH(A)-2OH-2	SH	16.0	1.96	0.237
SH(B)-2OH-2	SH	15.1	1.90	0.255

B. Structures and adsorption thermochemistry of reaction intermediates on GO

It is clear that GO usually contain both hydroxyl and epoxy groups in the graphene surface under O-rich and H-rich conditions [38]. In this section, we investigated the interaction of H_2S with GO with both epoxy and hydroxyl groups. In the case of adsorption of H_2S at the epoxy group of O-OH-1-gr structure, we first explored two initial adsorption modes (see Fig.3 (a) and (c)) the binding energy are calculated to be 11.6 and 11.1 kcal/mol, which is attributed to the electrostatic attraction, such as -O- and H−S−H, H−O- and H−S−H, and O−H- and SH_2. The H_2S dissociation

DOI:10.1063/1674-0068/28/cjcp1410187

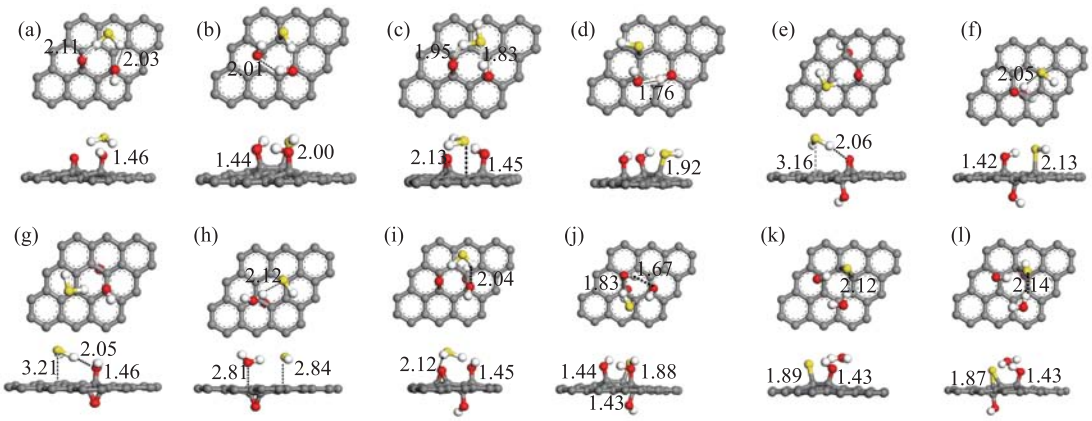

FIG. 3 Top and side view for the adsorption and dissociation of H_2S on graphene oxides containing both epoxy and hydroxyl functional groups. The red, gray, yellow, and white balls represent O, C, S, and H atoms, respectively. Distances are given in Å. (a) H_2S(A)-O-OH-1, (b) SH(A)-O-OH-1, (c) H_2S(B)-O-OH-1, (d) SH(B)-O-OH-1, (e) H_2S(A)-O-OH-2, (f) SH(A)-O-OH-2, (g) H_2S(B)-O-OH-2, (h) SH(B)-O-OH-2, (i) H_2S-O-2OH, (j) SH-O-2OH, (k) S-O-OH, and (l) S-O-2OH.

on the O-OH-1-gr structure are very similar to H_2S adsorption on GO with a single epoxy group, the S−H bond cleavage via H abstraction from H_2S, thus leads to epoxy ring opening. The calculated binding energy for the dissociated SH in Fig.3 (b) and (d) are 18.9 and 17.4 kcal/mol, respectively. From the above calculations, we also note the stabilities of GO after epoxy ring opening depend not only on the binding site of SH relative to the existing OH but also on the site of newly formed OH.

Figure 3 (e)−(h) shows the optimized structures of H_2S and SH adsorption on GO in which hydroxyl group attached to the neighboring carbon atom at the opposite side. The calculated binding energies for H_2S interaction with the epoxy group of O-OH-2-gr (denoted as H_2S(A)-O-OH-2) and with the hydroxyl (denoted as H_2S(B)-O-OH-2) are 9.4 and 10.3 kcal/mol, respectively. When H_2S interacts with the epoxide group, the H atom of H_2S move toward epoxide group of GO, leads to formation of C−S at GO (Fig.3(f)), however, when H_2S interacts with the hydroxyl group, the H atom abstractions from H_2S result in the H_2O formation and the SH desorption from GO (Fig.3(h)). It is interesting to notice that the presence of epoxy, dose not help to immobilize SH species. Figure 3 (i)−(l) show the optimized structures of H_2S, SH and S adsorption on GO with the combination of O-2OH-gr. We also identify model O-2OH-gr consisting of one -O- and two -OH- as the basic building blocks of low-energy GO for such composition. As shown Fig.3(i), the adsorptions of H_2S on O-2OH-gr with the two hydrogen atoms point to the oxygen atoms of GO, and the calculated binding energy is 13.8 kcal/mol. The H atom of H_2S moves toward epoxide group leading to epoxide group opening, result in C−S bond formation, illustrated in Fig.3(j), subsequently, the second H atom may abstract from SH to an existing OH group at the same side, which turns out the formation of H_2O as shown in Fig.3(l). Table II shows the calculated results for adsorption and dissociation of H_2S on GO containing both epoxy and hydroxyl functional groups. The binding energy results indicated that both epoxy and hydroxyl groups can enhance the binding of S to the C−C bonds and the effect of hydroxyl group is more local than that of the epoxy, it is mainly due to the induced ripples by the functional groups. But the value determined in this work, is slightly larger than that calculated for sulfur adsorption on GO [25], it can be understood by taking LDA functional in our calculations.

TABLE II The calculated binding energy (E_b in kcal/mol) and main parameters of key adsorbates on graphene oxides.

Structure	Adsorbate	E_b	d/Å	ΔQ/e
H_2S(A)-O-OH-1	H_2S	11.6	3.06	0.034
H_2S(B)-O-OH-1	H_2S	11.1	3.13	0.027
H_2S(A)-O-OH-2	H_2S	9.4	3.16	0.025
H_2S(B)-O-OH-2	H_2S	10.3	3.21	0.019
H_2S-O-2OH	H_2S	13.8	3.09	0.043
SH(A)-O-OH-1	SH	18.9	2.00	0.237
SH(B)-O-OH-1	SH	17.4	1.92	0.212
SH(A)-O-OH-2	SH	18.8	2.13	0.275
SH(B)-O-OH-2	SH	15.7	2.84	0.166
SH-O-2OH	SH	20.6	1.88	0.229
S-O-OH	S	36.8	1.89	0.364
S-O-2OH	S	42.0	1.87	0.385

C. Activation energy barriers

To further check whether the H_2S decomposed on GO surface, we calculated the barriers for its S−H bond

DOI:10.1063/1674-0068/28/cjcp1410187

cleavage on GO. Figure 4 shows a series of reaction pathways for H abstraction from H_2S on different GO models, together with an energy variation along the reaction coordinate. From Fig.4(a), H_2S can dissociate into SH species located at the A site (see Fig.2(a)) by overcoming a barrier of 15.5 kcal/mol, in parallel to its dissociation located at the B sites, need to overcome a barrier of 16.3 kcal/mol, this observation indicates that such ring opening of the epoxy group with H_2S is kinetically more favorable. The corresponding dissociation energy value of H_2S for site A is −7.0 kcal/mol, larger than the −0.6 kcal/mol of site B. The results show us that the ring opening of epoxides can be facilitated by H_2S. For GO including a 1,2-hydroxyl group pair (Fig.4(b)), the dehydrogenation reactions of H_2S are promoted due to the lower barriers compared with the case of one epoxy group. The relatively lower barriers has also been found in NH_3 dissociation on GO [21]. This is mainly because the initial state with adsorption of H_2S at the carbon atom neighboring the hydroxyl group pair will form a 4-fold coordinated N atom structures, so the presence of another OH group at the opposite side relative to the adsorbed H_2S activates the oxygen group to facilitate OH hydrogenation. Figure 4(c) show relative energy profiles for adsorption and dissociation of H_2S on O-OH-2-gr, the predicted barrier height of 5.2 kcal/mol, which is noticeably lower than 15.5 kcal/mol estimated for the single epoxide case, due to activation by opposite hydroxyl group. Figure 4 (d) and (e) show relative energy profiles for dissociation from H_2S to S on O-OH-1-gr and O-2OH-gr, respectively. In two reaction process, the first step is H atom of H_2S prior to attack the epoxide group rather than the hydroxyl group kinetically because hydroxyl group activate ring opening of the epoxy group. The next step, we found that H of SH species may be abstracted by a nearby hydroxyl, leading to S bound to C−C bridge site and formation of H_2O, simultaneously. For H_2S adsorption and dissociation on O-OH-1-gr, this process are exothermic 7.3 and 23.2 kcal/mol for formation of the OH group and H_2O (Fig.4(d)) with respect to the initial states, respectively. By contrast with Fig.4(d), the relatively facile H abstraction for H_2S-O-2OH system (Fig.4(e)) is not surprising considering hydroxyl attach to the opposite side. From our calculations, the calculated barrier height of 5.8 and 2.5 kcal/mol in Fig.4(e) is noticeably lower than that of Fig.4(d). The present results provide OH on GO can promote S−H bond breaking and low reaction barrier.

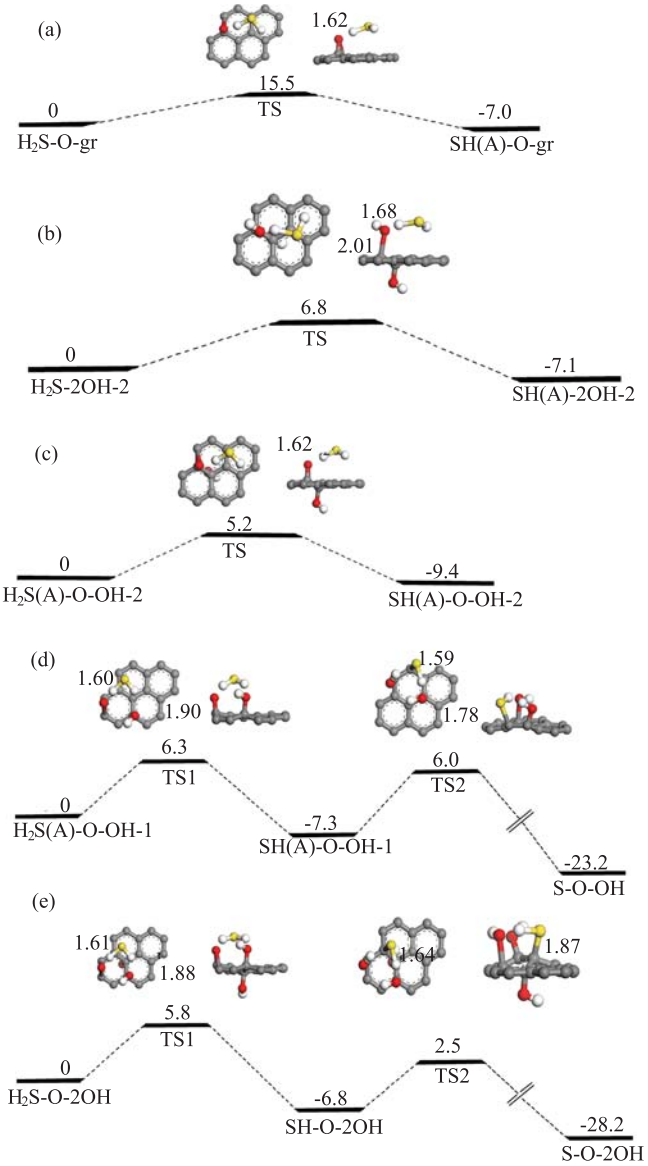

FIG. 4 The decomposition of H_2S molecule on graphene oxides and the calculated potential energy profiles given in kcal/mol. (a) H_2S-O-gr, (b) H_2S-2OH-2, (c) H_2S(A)-O-OH-2, (d) H_2S(A)-O-OH-1, and (e) H_2S-O-2OH.

D. Reaction mechanism

By mapping out the above reaction network, we have estimated the most favorable channel for H_2S dissociation into S. Figure 5(a) is optimized configurations for the initial (IS), transition (TS), intermediate (INT) and final (FS) states of H abstraction from HS species together with corresponding activation energy. As illustrated in Fig.5, the epoxide group was opened via H atom abstraction from H_2S, the H atom of the OH group pointed to the S atom of SH because of the formation of weak hydrogen bond. If the second H atom transfer from SH to the O of OH, the OH- along the C−O axis and SH- along C−S should simultaneously rotate and close to each other. For a further understanding of the reaction mechanism, we introduced intermediate states SH-2OH-INT by rotating the SH group along the C−S bond. Because the calculated energy barrier is only 3.2 kcal/mol, this change from states SH-2OH-IS to SH-2OH-INT states is easily achieved. Considering the OH and SH groups of SH-2OH-IS are close each

DOI:10.1063/1674-0068/28/cjcp1410187

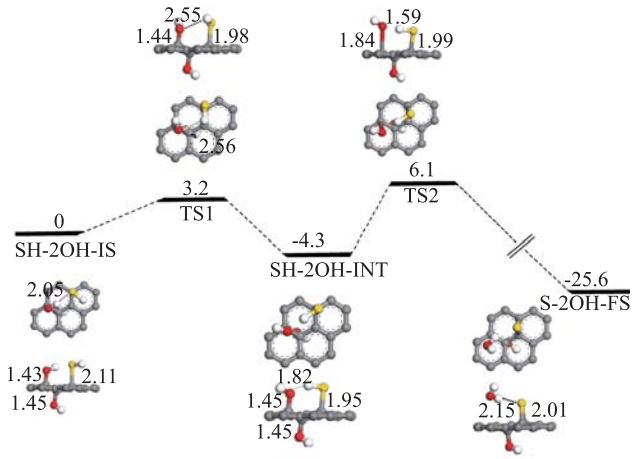

FIG. 5 Optimized configurations for the initial (IS), transition (TS), intermediate (INT) and final (FS) states of H abstraction from HS species together with corresponding activation energy and exothermicity (kcal/mol). The bond length are given in Å.

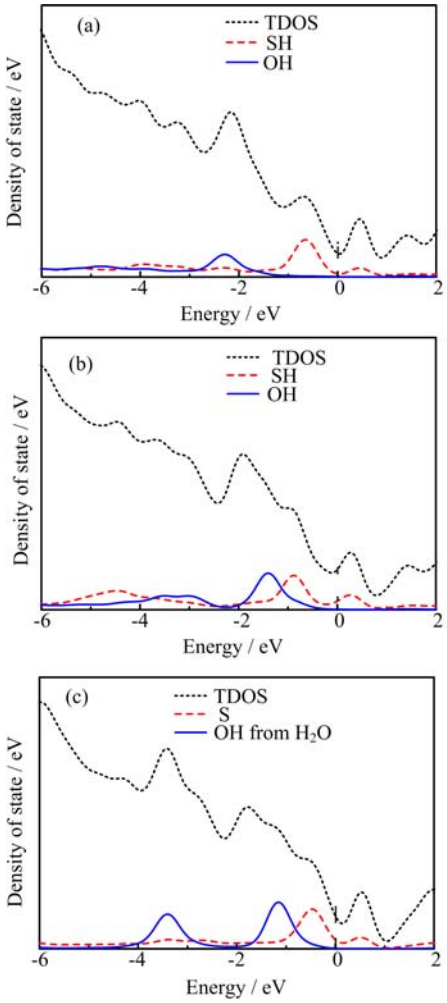

FIG. 6 The density of states of (a) SH-2OH-IS, (b) SH-2OH-INT, and (c) S-2OH-FS.

other, the O atom can approach the H of SH with a distance of 1.95 Å after OH rotation. According to our calculations, SH dissociation from INT to FS states has a reaction barrier of 10.4 kcal/mol, resulting in OH hydrogenation. Thus, the pathway is the favorable reaction path, and the second H transfer is the rate-determining step in the whole reaciton process.

To gain more insight into the reaction mechanism for dissociation of H_2S on graphene oxide, the total density of states (TDOS) and the projected density of states (PDOS) of SH-2OH-IS, SH-2OH-INT and S-2OH-FS are shown in Fig.6 (a)−(c), respectively. TDOS of SH-2OH-IS, SH-2OH-INT, and S-2OH-FS reveal that all systems are semiconductors with different band gaps, consistent with the energy gap of graphene tuning by functionalization with other impurities. From SH-2OH-IS to SH-2OH-INT state, the OH orbitals are gradually broadened and involved within S3p orbital, giving rise to charge from the S atom to GO, thus leading to the second H atom of SH abstraction. In Fig.6(c), it is found that the electron states of OH from H_2O are localized at energy −1.6 and −3.5 eV, indicating OH desorption from graphene nanosheet. In light of the above discussion, we conclude that H_2S dissociation on GO is firstly determined by epoxide ring open, and the second H transfer is the rate-determining step in the whole reaciton process. Furthermore, the relatively facile H abstraction due to low energy barrier is observed when GO contains unreacted hydroxyl groups.

IV. CONCLUSION

Using periodic density functional theory, we have studied H_2S adsorption and dissociation on graphene oxide nanosheet. The comprehensive reaction network of H_2S oxidation with epoxy and hydroxyl groups of GO was discussed. The calculation results show that the reduction reaction is mainly governed by epoxide ring opening and hydroxyl hydrogenation which is initiated by H transfer from H_2S or its derivatives. Furthermore, the presence of another OH group at the opposite side relative to the adsorbed H_2S activates the oxygen group to facilitate epoxide ring opening and hydroxyl hydrogenation. For H_2S interaction with -O and -OH groups adsorption on each side of graphene, the reaction pathway is the favorable reaction path by the introduction of intermediate states, the calculated energy barriers were 3.2 and 10.4 kcal/mol, respectively, which is corresponding to rotation of the SH and the second hydrogen abstraction, thus the second H transfer is the rate-determining step in the whole reaciton process. In addition, our calculations indicate that both epoxy and hydroxyl groups can enhance the binding of S to the C−C bonds and the effect of hydroxyl group is more local than that of the epoxy. Present results

DOI:10.1063/1674-0068/28/cjcp1410187

provide a basis for further experimental and theoretical exploration of S-containing compounds adsorption and dissociation on graphene oxides surface.

V. ACKNOWLEDGMENTS

This work was supported by the National Natural Science Foundation of China (No.21004009) and the Foundation of Jiangxi Educational Committee (No.GJJ13447 and No.GJJ14485). We are grateful to High Performance Computer Center of State Key Laboratory of Physical Chemistry of Solid Surface (Xiamen University).

[1] A. K. Geim, Science **324**, 1530 (2009).
[2] C. N. R. Rao, A. K. Sood, K. S. Subrahmanyam, and A. Govindaraj, Angew. Chem. Int. Ed. **48**, 7752 (2009).
[3] K. R. Ratinac, W. Yang, S. P. Ringer, and F. Braet, Environ. Sci. Technol. **44**, 1167 (2010).
[4] S.Tang and Z. X. Cao, J. Chem. Phys. **131**, 114706 (2009).
[5] J. Andzelm, N. Govind, and A. Maiti, Chem. Phys. Lett. **421**, 58 (2006).
[6] D. C. Elias, R. R. Nair, T. M. G. Mohiuddin, S. V. Morozov, P. Blake, M. P. Halsall, A. C. Ferrari, D. W. Boukhvalov, M. I. Katsnelson, A. K. Geim, and K. S. Novoselov, Science **323**, 610 (2009).
[7] J. O. Sofo, A. S. Chaudhari, and G. D. Barber, Phys. Rev. B **75**, 153401 (2007).
[8] N. Lu, Z. Li, and J. Yang, J. Phys. Chem. C **113**, 16741 (2009).
[9] S. Tang and S. Zhang, J. Phys. Chem. C **115**, 16644 (2011).
[10] S. Myung, J. Park, H. Lee, K. S. Kim, and S. Hong, Adv. Mater. **22**, 2045 (2010).
[11] S. Wang, J. Pu, D. S. H. Chan, B. J. Cho, and K. P. Loh, Appl. Phys. Lett. **96**, 143109 (2010).
[12] O. C. Compton and S. T. Nguyen, Small **6**, 711 (2010).
[13] Y. Zhu, S. Murali, W. Cai, X. Li, J. W. Suk, J. R. Potts, and R. S. Ruoff, Adv. Mater. **22**, 3906 (2010).
[14] Z. Wei, D. Wang, S. Kim, S. Y. Kim, Y. Hu, M. K. Yakes, A. R. Laracuente, Z. Dai, S. R. Marder, C. Berger, W. P. King, W. A. Heer, P. E. Sheehan, and E. Riedo, Science **328**, 1373 (2010).
[15] K. P. Loh, Q. Bao, and G. E. M. Chhowalla, Nat. Chem. **2**, 1015 (2010).
[16] X. F. Gao, J. Jang, and S. Nagase, J. Phys. Chem. C **114**, 832 (2010).
[17] D. Li, M. B. Muller, S. Gilje, R. B. Kaner, and G. G.Wallace, Nat. Nanotechnol. **3**, 101 (2008).
[18] M. J. Fernandez-Merino, L. Guardia, J. I. Paredes, S. Villar-Rodil, P. Solis-Fernandez, A. Martinez-Alonso, and J. M. D. Tascon, J. Phys. Chem. C **114**, 6426 (2010).
[19] W. F. Chen, L. F. Yan, and P. R. Bangal, J. Phys. Chem. C **114**, 19885 (2010).
[20] S. Pei, J. Zhao, J. Du, W. Ren, and H. Cheng, Carbon **48**, 4466 (2010).
[21] S. B. Tang and Z. X. Cao, J. Phys. Chem. C **116**, 8778 (2012).
[22] H. P. Ling, P. Simek, Z. Sofer, and M. Pumera, Nano Lett. **6**, 5262 (2013).
[23] Y.Yan, Y. X. Yin, S. Xin, Y. G. Guo, and L. J. Wan, Chem. Commun. **48**, 10663 (2012).
[24] J. Z. Wang, L. Lu, M. Choucairc, J. A. Stridec, X. Xua, and H. K. Liu, J. Power Sources **16**, 7030 (2011).
[25] L. Ji, M. Rao, H. M. Zheng, L. Zhang, Y. C. Li, W. H. Duan, J. H. Guo, E. J. Cairns, and Y. G. Zhang, J. Am. Chem. Soc. **133**, 18522 (2011).
[26] Y. Cao, X. Li, I. A. Aksay, J. Lemmon, Z. Nie, Z. Yang, and J. Liu, Phys. Chem. Chem. Phys. **13**, 7660 (2011).
[27] J. Wang, J. Chen, K. Konstantinov, L. Zhao, S. H. Ng, G. X. Wang, Z. P. Guo, and H. K. Liu, Electrochim. Acta **51**, 4634 (2006).
[28] J. Wang, S. Y. Chew, Z. W. Zhao, S. Ashraf, D. Wexler, J. Chen, S. H. Ng, S. L. Chou, and H. K. Liu, Carbon **46**, 229 (2008).
[29] L. X. Yuan, J. K. Feng, X. P. Ai, Y. L. Cao, S. L. Chen, and H. X. Yang, Electrochem. Commun. **8**, 610 (2006).
[30] X. Liang, Z. Wen, Y. Liu, H. Zhang, L. Huang, and J. Jin, J. Power Sources **196**, 3655 (2011).
[31] S. R. Chen, Y. P. Zhai, G. L. Xu, Y. X. Jiang, D. Y. Zhao, J. T. Li, L. Huang, and S. G. Sun, Electrochim. Acta **56**, 9549 (2011).
[32] B. H. Jeon, J. H. Yeon, K. M. Kim, and I. J. Chung, J. Power Sources **109**, 89 (2002).
[33] B. Delley, J. Chem. Phys. **92**, 508 (1990).
[34] J. P. Perdew and Y. Wang, Phys. Rev. B **45**, 13244 (1992).
[35] D. Svetla, E. Schroder, B. I. Lundqvist, and D. C. Langreth, Phy. Rev. Lett. **96**, 146107 (2006).
[36] X. Gao, Y. Zhao, B. Liu, H. Xiang, and S. B. Zhang, Nanoscale **4**, 1171 (2012).
[37] X. Gao, Y. Wang, X. Liu, T. L. Chan, S. Irle, Y. Zhao, and S. B. Zhang, Phys. Chem. Chem. Phys. **13**, 19449 (2011).
[38] W. Cai, R. D. Piner, F. J. Stadermann, S. Park, M. A. Shaibat, Y. Ishii, D. Yang, A. Velamakanni, S. J. An, M. Stoller, J. An, D. Chen, and R. S. Ruoff, Science **321**, 1815 (2008).

DOI:10.1063/1674-0068/28/cjcp1410187